Title

Short-term post-wildfire dry-ravel processes in a chaparral fluvial system

Authors

Florsheim, Joan L
Chin, Anne
O'Hirok, Linda S
et al.

Publication Date

2015-04-01

DOI

10.1016/j.geomorph.2015.03.035

Peer reviewed

Short-term post-wildfire dry-ravel processes in a chaparral fluvial system

Joan L. Florsheim, Anne Chin, Linda S. O'Hirok, Rune Storesund

Abstract

Dry ravel, the transport of sediment by gravity, transfers material from steep hillslopes to valley bottoms during dry conditions. Following wildfire, dry ravel greatly increases in the absence of vegetation on hillslopes, thereby contributing to sediment supply at the landscape scale. Dry ravel has been documented as a dominant hillslope erosion mechanism following wildfire in chaparral environments in southern California. However, alteration after initial deposition is not well understood, making prediction of post-fire flood hazards challenging. The majority of Big Sycamore Canyon burned during the May 2013 Springs Fire leaving ash and a charred layer that covered hillslopes and ephemeral channels. Dry-ravel processes following the fire produced numerous deposits in the hillslope-channel transition zone. Field data focus on: 1) deposition from an initial post-wildfire dry-ravel pulse; and 2) subsequent alteration of dry ravel deposits over a seven-month period between September 2013 and April 2014. We quantify geomorphic responses in dry ravel deposits including responses during the one small winter storm that generated runoff following the fire. Field measurements document volumetric changes after initial post-wildfire deposition of sediment derived from dry ravel. Erosion and deposition mechanisms that occurred within dry-ravel deposits situated in the hillslope-channel transition zone included: 1) mobilization and transport of a portion or the entire deposit by fluvial erosion; 2) rilling on the surface of the unconsolidated deposits; 3) deposition on deposits via continued hillslope sediment supply; and 4) mass wasting that transfers sediment within deposits where surface profiles are near the angle of repose. Terrestrial LiDAR scanning point clouds were analyzed to generate profiles quantifying depth of sediment erosion or deposition over remaining dry ravel deposits after the first storm season. This study contributes to the understanding of potential effects of wildfire on fine sediment delivery to fluvial systems in chaparral ecosystems.

Keywords: Dry ravel; Wildfire; Chaparral; Hillslope erosion

Corresponding author email: florsheim@eri.ucsb.edu

1. Introduction

Dry ravel, the transport of sediment primarily under the force of gravity, transfers weathered sediment from hillslopes to channels. Dry ravel is a dominant sediment transport process in steep chaparral regions (Krammes, 1965; Rice, 1974; 1982) where slope is greater than the angle of repose (Lamb et al, 2011). Early research showed high sediment flux rates on steep chaparral slopes (Anderson, et al., 1959; Krammes, 1965). In southern California's Transverse Ranges, where slopes often exceed 31˚, hillslope stability is aided by chaparral vegetation between wildfires (Florsheim et al., 1991). On such steep slopes, weathered sediment may be stored upslope of vegetation whose trunks and branches form barriers to downslope sediment transfer. During and after wildfire, sediment stored behind burned vegetation is destabilized; thus, wildfire that burns chaparral vegetation and the organic litter layer acts as an agent to increase surface erosion rates (Florsheim et al., 1991; Gabet, 2003; Lave and Burbank, 2004; Roering and Gerber, 2005; Shakesby and Doerr, 2006; Jackson and Roering, 2009; Lamb et al, 2011; 2013; DiBiase and Lamb, 2013). Sediment transported downslope by dry ravel collects in hillslope depressions or forms irregular or inverted cone-shaped deposits at the base of hillslopes near channel margins (Florsheim et al., 1991).

It is well understood that most material contributed by dry ravel is transported down hillslopes during or immediately after the wildfire; thus, the effect of wildfire on hillslope sediment flux may be significant. Therefore, consideration of wildfire in landscape evolution models to predict landform response to climate and tectonic changes has recently been addressed (Benda and Dune, 1997; Gabet and Dunne, 2003; Lave and Burbank, 2004; Roering and Gerber, 2005; Lamb et al., 2011). For example, Lamb et al. (2011) developed a mass balance-continuity model for sediment storage by vegetation barriers on steep hillslopes to predict hillslope sediment yield following wildfire. In the model, the volume of sediment stored on hillslopes is a function of chaparral vegetation density, capacity of plants to impound sediment, and the contributing hillslope area. As noted by Lamb et al. (2011), in models developed by Roering and Gerber (2005) and Gabet (2003), the dry-ravel flux predicted is infinite when slope is greater than the angle of repose, such that on steep slopes without vegetation, flux is limited by supply. Therefore, it is critical to consider the time needed to establish vegetation between fires, the time needed for bedrock to weather and replenish hillslope stored sediment, and the fire recurrence interval. Further, as global warming has increased spring and summertime temperatures and the length of the dry season in the western United States, wildfire activity has increased (Westerling et al., 2006). However, Lamb et al. (2011) suggest that even if fire frequency increases as projected, hillslope production of weathered material would be a factor limiting sediment supply.

Dry-ravel processes are a significant wildfire-related process in semi-arid environments because, unlike many post-fire erosional responses that occur during large storms, dry ravel contributes sediment to channels during the dry season regardless of whether subsequent storms are large or small or if climatic patterns reflect a wet or dry cycle. Dry ravel has been widely reported in chaparral Mediterranean climates (Shakesby and Doerr, 2006), and the need to understand dry ravel becomes more relevant with increased aridity (Moody et al., 2013). Because of the projected increase in the frequency of wildfire, understanding processes affecting dry-ravel deposits is an important research problem.

Despite the growing understanding of dry-ravel dynamics and its role landscape evolution, little is known about sediment dynamics and geomorphic modifications on dry ravel deposits after their initial deposition—especially during drought periods when these ephemeral deposits may persist in the hillslope channel margin transition zone for longer periods of time. In this paper, we document post-fire changes in a burned basin in southern California's Transverse Ranges where dry ravel is a dominant post-wildfire process. We used detailed field measurements and terrestrial LiDAR scanning, (TLS) to document geomorphic changes within dry ravel deposits during a seven month period following initial deposition, a period spanning the first summer and winter following wildfire. The results advance understanding of how dry ravel deposits contribute to sediment yield in steep chaparral environments – an important factor in the evolution of these landscapes.

2. Study Area

The majority of Big Sycamore Canyon (drainage area ~55 km^2; Figure 1) burned during the May 2013 Springs Fire. The canyon is situated in the western portion of the Santa Monica Mountains, the southern-most range within California's east-west trending Transverse Ranges. Elevations range from 846 m in the headwaters to sea level where Big Sycamore Creek joins the Pacific Ocean. The Santa Monica Mountains are composed of Cenozoic sedimentary rocks; the study area within the Lower Topanga Formation is primarily composed of layered marine shale beds inter-bedded with sandstone (Yerkes and Campbell, 1980; Dibblee and Ehrenspeck, 1990a; 1990b; Yerkes et al., 2005).

The semi-arid Mediterranean climate of southern California is characterized by a long dry season and a relatively short wet season such that ~90% of the annual rainfall occurs between November and April. The study area is currently affected by a drought that began in 2012 and

that is influencing the western USA. Little rain fell in the study area during water year 2012 and dry conditions continued through 2013 (Figure 2). Vegetation in Big Sycamore Canyon is dominated by chaparral, which is adapted to the long dry season in southern California in elevation zones above ~250 m (O'Leary, 1981). Chaparral vegetation includes a diverse assemblage of evergreen and drought-tolerant shrubs that are resilient to wildfires. Some plants resprout from root systems and burls and others, such as short-lived annuals, require fire to germinate seeds (Quinn and Keeley, 2006). The riparian zone along the ephemeral main channel in Big Sycamore Canyon contains sycamore, willow, and oak trees along with chaparral shrubs and herbaceous plants.

Wildfires are especially common in the southern California chaparral during the late summer to early fall when easterly "Santa Ana" winds produce hot dry conditions (Mortiz et al., 2010). However, the Springs Fire occurred during May 2-6, 2013 and was driven by early-season Santa Ana winds. The springtime fire burned ~100 km^2 including 85% of Big Sycamore Canyon (NPS, 2013). The fire burned hillslope chaparral vegetation and trees within the riparian zone. Following the fire, ash and a charred layer covered hillslopes as well as the dry tributary channels and the main channel. During the fire and dry summer following the Springs Fire, active dry-ravel processes produced numerous deposits that merged at the base of hillslopes at the margins of stream channels. Only one small runoff-generating storm on February 28-March2, 2014 interrupted the drought during water year 2014 (Figure 3).

The study reach investigated in Big Sycamore Canyon following the Springs Fire is ~180 m in length and lies within an area previously investigated by Chin (1999; 2002) (Figure 1). The study reach, Klein Reach (*Reach A*), is characterized by a relatively steep gradient (~2.5˚) and is covered by coarse boulder-sized material, that results in prominent step-pool sequences (Chin, 1999). Characteristics of burned hillslopes adjacent to the study reach include steeper gradients on the north side of the valley (~27˚) than on the south side (~15˚). Inter-bedded shale and sandstone bedrock are exposed on the steeper slopes. Two first-order tributaries emanating from the north join Big Sycamore Creek in the study reach.

3. Methods

A range of field methods was employed to investigate changes in dry ravel deposits formed at the hillslope-channel transition in Big Sycamore Canyon following the Springs Fire. Two field campaigns were conducted: 1) in September 2013 after the wildfire but before the only winter storm that generated runoff; and 2) following the February 28-March 2, 2014 storm. Each time, field data collection in the study reach included two separate data sets: 1) detailed field

measurements of dry-ravel deposit volume using conventional measuring techniques; and 2) surface profiles of dry ravel deposits generated from TLS point cloud data to illustrate changes resulting from erosion and depositional processes in dry ravel deposits. We assumed that measurements made in September 2013 represented baseline conditions following the wildfire, e.g. conditions at this time reflect post-fire erosion of hillslopes by the process of dry ravel and deposition of this material along channel margins.

3.1 Field measurements of dry ravel deposit volume

Field measurement of dry ravel deposits included height (*h*) from the base of the deposit in the channel to the top on the hillslope and length (*l*) along the longitudinal profile of the channel using a stadia rod and tape measure, respectively. In order to differentiate pre-and post-wildfire deposition from dry ravel processes, we assumed that when probed, resistance to penetration was assumed to reflect the ground surface prior to deposition of material by dry ravel following the Springs Fire. Depth (*d*) of each deposit was measured perpendicular to height using a rebar probe. Thus, we inferred that any older material present before the fire would be noticeably difficult to penetrate. Data collected in September 2013 included 23 individual ravel deposits in Klein Reach (*Reach A*). We repeated the geometric measurements in March 2014 following the winter storm season to document observable changes in dry-ravel deposit morphology and volume. The surficial median grain size of ravel deposits was measured from clasts present on three ravel deposits from Klein Reach (*Reach A*). Methods to calculate volume of each individual deposit for each period used geometric relationships depending on morphologic character, or shape of the deposit, generalized as inverted (e.g. upside-down orientation) cones or rectangles which sometimes appear to be coalesced cones or other irregular shapes (Figure 4a and 4b). Volumes of deposits shaped like inverted cones were estimated as one half the volume of a cone (V_{ci}):

$$V_{ci} = (1/6)\,\pi\, r^2\, h \qquad (1)$$

where depth, measured in the location corresponding to the deepest portion of the deposit using a steel rebar probe, replaces the cone radius, *r*. Volumes of individual deposits shaped like quasi-rectangles (V_{ri}) were estimated as the product of the surface area of the deposit ($w\,h$) and depth, where height was measured in several locations along the length of the deposit with the stadia rod, and with depth averaged from corresponding measurements:

$$V_{ri} = A\,d \qquad (2)$$

Summing these changes yields the total volume V_T of sediment stored in the *n* dry-ravel deposits for the reach:

$$V_T = \sum V_{ci} + \sum V_{ri} \qquad i = 1...n \qquad (3)$$

A corresponding total rate (q_T) of sediment deposition of the dry-ravel deposits was calculated as:

$$q_T = 1/\Delta t \; V_T \qquad (4)$$

where Δt is the period between the fire and measurement . It is likely that the majority of this material was deposited during the fire or within the first month after the fire (Florsheim et al., 1993; Lamb et al., 2013).

3.2 Terrestrial LiDAR scanning (TLS) profiles

More detail with respect to morphologic changes in dry ravel deposits was afforded by comparing profiles created using TLS point cloud data surveyed during two campaigns, September 2013 and April 2014 conducted in Klein Reach (*Reach A*). We utilized this profile approach because shadows caused by (burned) branches between the scanner and dry ravel deposits and the growth of a dense herbaceous layer in some areas two-weeks prior to collection of the April 2014 scan. Thus, the collected TLS data set did not have sufficient point coverage/resolution to generate a high-resolution Triangulated Irregular Network (TIN) surface by which to analyze volumetric changes in deposits between the 2013 and 2014 scan campaigns.

TLS field data collection consisted of three primary steps: site reconnaissance and control establishment, deployment of targets to link individual scans together in a composite point cloud, and finally performing the suite of scans along the channel reach of interest. The site reconnaissance provided the basis by which to configure the scan setup locations and general target distribution to facilitate point cloud registration. GPS receivers were used and configured to acquire satellite data for subsequent Online Positioning User Service (OPUS; http://www.ngs.noaa.gov/OPUS/) solutions provided by the National Geodetic Survey to establish datum control. Following the site reconnaissance, physical targets were placed throughout the scan area. Following the initial distribution of physical targets, TLS initiated using a Riegl VZ-400 scanner included 14 scan positions over a channel distance of ~180 m (Figure 5). One scan was completed per setup location.

Point density of the terrain surface within a point cloud is a function of distance of the physical feature from the scanner, topographic complexity of the terrain, and the presence of

barriers such as vegetation between scanner and the terrain. The point density (within 1.0 cm of the profile lines) ranged between ~10,000 points/m^2 and ~280,000 points/m^2, with an average point density of 65,000 points/m^2.

Registration of the 2013 and 2014 scans followed a method described by Williams et al. (2012). Point density was not a consideration as part of the registration process; rather, the distance between scan setup locations was the controlling factor for point density. Field data were imported into RiSCAN PRO v1.8.0 for registration. The registration process aligns individual point clouds scanned from each set up position into an aggregate master point cloud. Targets together with physical features were used in our registration scheme. The datasets were registered (alignment of the individual scans into an aggregate point cloud) using the "Coarse" and "Multi-Station Adjustment" (MSA) Registration routines. The 2014 data were aligned with the 2013 data by importing the 2014 data into the same Riegl RiScan project as the 2013 data. A standard target alignment was then applied to this dataset; the 2014 data were then treated as a rigid body, and this body was manually moved into an approximate alignment with the 2013 dataset to seed the MSA routine. For alignment purposes, the point clouds were temporarily filtered to remove areas where excess changes would have taken place (such as upper tree branches); the MSA was performed holding the 2013 data fixed, and assigning a higher weighting to the target alignment of the 2014 dataset. Essentially, this results in each individual scan from 2014 to be fit to all scans from 2013, while still allowing targets in the 2014 dataset to be used to hold the rigid body accuracy that had already been obtained based on target alignment of the 2014 dataset. Thereafter, registration to refine alignment of the individual dry ravel deposits for comparison between the September 2013 and April 2014 scans was accomplished within Maptec I-Site Studio (process and modeling) software using fixed objects such as large boulders as guides. Because of the high point cloud density, a high accuracy matching could be achieved.

To generate the 2013 and 2014 surface profiles parallel to the measured height of each dry ravel deposit (see section 3.1) over the dry ravel deposits, we used Maptec I-Site Studio to isolate point cloud data. To scale the extracted point cloud data for comparison of the 2013 and 2014 scans, the xyz coordinates of the upper and lower ends of a projected line were used for plotting in technical graphics software. Profile lines were drawn by eye though the lowest points in the point cloud data (along the profile selected)—with data magnified so that individual points were visible. Using this graphical method, we then quantified elevation changes along the dry ravel deposit profiles where negative and positive changes represent surficial erosion or deposition, along the dry ravel deposit profiles derived from the respective TLS point clouds. Thus, we enhance our field measurements of changes in dry ravel deposit volume and observations of processes such as rills, undercutting, and mass wasting by

complementing the field measurements with analysis of TLS data to quantify small morphologic changes within the ravel deposits that occurred during the same period.

3.4 Errors and uncertainty

The primary error introduced into the data set during TLS data collection is the error of the scanning unit. The reported error for the Riegl VZ-400 at a distance of 100 m is 5 mm (http://www.riegl.com/uploads/tx_pxpriegldownloads/10_DataSheet_VZ-400_2014-09-19.pdf); however, the distances between scanner setups in our investigation were much less; the scanner was set up at distances of ~9 m apart on average in the upstream portion of the study reach where the majority of the dry ravel deposits formed (Figures 5 and 6). Larger distances between scanner set ups in the downstream portion of the reach prevented TLS analysis of some of the dry ravel deposits.

Detected erosion and deposition was based on physical differences between the 2013 and 2014 TLS scanned point cloud data, with the physical configuration of the topography captured by the point cloud. Our analyses directly used the point cloud (no filtering or post-processing such as TIN surfacing or interpolation), which enabled us to make high-precision measurements, with error equivalent to primary instrument error. Because both the average point density along the profiles and the density of points used to generate the profiles are high, we are confident that the detected changes in elevation of the 2013 and 2014 profiles generated through their respective point clouds represent real change, not error. However, some uncertainty could arise from the method used to draw the profiles from the point cloud data. To minimize this error, horizontal separation of points along the profile greater than 0.1 m was considered to be a data gap and portions of profiles that exceeded this gap length were not included in the comparison of the 2013 and 2014 profiles.

All data were initially processed using WGS84 geocentric coordinates, which are true raw point positions with no applied projection; therefore, no error is introduced in this step. Conversion to UTM was done using the Blue Marble Geographic Calculator. Delineating the WGS84 positions of the data within the point cloud was accomplished using the OPUS solutions. The primary errors introduced into the dataset during registration are (1) errors in target overlap and positioning, which are on the order of 5 to 10 mm, and (2) errors in the OPUS solution. Because the 2014 data set is 'fit' to the 2013 dataset, the errors associated with the OPUS solution do not apply to the aligned 2013-2014 point clouds, but rather are relevant only if the point cloud is subsequently compared against an unrelated data set. Following registration, the point cloud files were exported (in *.las format) for post-processing using

Maptek's Isite-Studio to correct remaining error. Because the scans were already aligned in geocentric coordinates, and then converted, any introduced error is negligible.

Other potential sources of uncertainty in the analysis of the TLS point cloud data occurred because of a dense herbaceous vegetation layer that existed on some of the deposits. To minimize error in comparison of the 2013 and 2014 profiles: 1) profile locations were selected to minimize the presence of vegetation; and 2) deposits (or portions of deposits) with dense leafy vegetation growth between the two field campaigns were excluded from analysis. Moreover, in channel margin areas where irregular topography, in relation to scanner position, created data gaps or low point density, the deposits were not included in the analysis.

4. Results

4.1 Dry ravel deposition following wildfire

Weathered sediment was contributed by dry-ravel processes to the hillslope-channel transition zone in Big Sycamore Canyon following the 2013 Springs Wildfire forming irregularly spaced deposits along the margins of the channel (Figure6). **T**he majority (17 of 23) of deposits formed at the base of the steeper northern hillslope. Morphology is grouped in two main shapes, inverted cones or irregular, quasi-rectangular shapes (see Figure 4a and 4b). About 56% of the post-fire dry-ravel deposits formed in the study reach had inverted cone-shaped morphology. Field observation suggests that such cones often form when there is a distinct and sometimes worn pathway on the lower hillslope above the deposit that focuses sediment transported toward the valley bottom during dry ravel. The remaining deposits have irregular, quasi-rectangular shapes. We infer that such irregular deposits form when hillslope-sediment pathways are more dispersed or when multiple deposits coalesce. The median grain size of sediment contributed by dry ravel processes to Klein Reach (*Reach A*) ranged between 3 mm and 11 mm (Figure 7).

4.2 Change in dry ravel deposit storage

The volume of sediment in individual deposits within the study reach (Table 1) was summed to quantify the post-wildfire reach-scale volumetric sediment contribution from dry ravel, V_T = 11.9 m^3/m and the volume stored per unit length of channel (0.7 m^3/m). A reduction in V_T of ~33% of the post-fire dry ravel deposits occurred between the September 2013 and April 2014 field campaigns, which corresponds to a decrease of ~0.02 m^3/m longitudinally along the channel.

The reduction of volume stored in dry ravel deposits is attributed to several erosion processes that occurred during the one small runoff-generating storm on February 28-March2, 2014. Of the total volume of sediment eroded from dry ravel deposits during the storm, about 31% can be attributed to erosion of the entire or majority of the volume of 6 of 23 deposits. This volume corresponds to ~10% of the total volume of material deposited following the post-wildfire measured in 2013. Field observations identified additional processes that contributed to the reduction of sediment stored in dry ravel (Figure 8a and 8b) such as: undercutting at the base of a deposit by fluvial erosion (4 of 23 deposits), small rills formed in the surface of deposits (3 of 23 deposits), and small mass wasting failures in the surface of the deposits.

Detailed quantitative analysis of individual dry-ravel deposits derived from profiles constructed using the TLS point cloud data allow quantification of erosion and/or deposition of sediment along the same profile at sub-centimeter levels of accuracy (Figure 9a and 9b; Figure 10). Sixteen of the 23 deposits were analyzed to compare 2013 to 2014 ravel surface profiles. One densely vegetated deposit (A15) was not included in the TLS analysis. Portions of profiles with data gaps resulting from shadows caused by irregular topography of the channel margins in relation to the scanner position were not included in the analysis.

Dry-ravel deposit surface-profile slopes range from 25° to 45°, with an average of 33°—close to the angle of repose. Accordingly, most profiles exhibit both erosional and depositional changes along their lengths. On average ~26% of the profile lengths measured indicated net erosion, whereas ~31% indicated net deposition during the seven month period—the remainder exhibit no change. Measured depths of erosion and deposition along profile surfaces exceed a threshold of resolution of 0.005 m. Measured depths of erosion range from 0.012 m to 0.054 m and depths of deposition are similar in magnitude with a range from 0.015 m to 0.063 m (Table 2). A dimensionless deposition index is defined as the depth of deposition per unit length of the deposit whereas the erosion index is defined as the depth of erosion per unit length of the deposit. Longitudinally from the upper to lower portion of the surface profiles, the deposition index averages 0.115 m/m whereas the erosion index averages 0.056 m/m.

5. Discussion

5.1 Dry ravel deposit volume

Sediment derived from wildfire-related dry ravel processes represents an important component of basin sediment yield. In the steep chaparral terrain characterizing Big Sycamore Canyon, quantifying short-term post-wildfire sediment delivery to the fluvial system adds to our understanding of post-wildfire sediment dynamics. This in turn, is important in understanding the magnitude and rate of processes that inform models of landscape evolution. Post-wildfire

sediment contribution by dry-ravel processes is spatially variable. This study, conducted in the Klein Reach (Reach A) of Big Sycamore Canyon reports 0.07 m^3/m, a relatively low value for the volume of sediment contributed along the margins of the ephemeral channel. This value is ~30% of that measured farther downstream where dry-ravel deposition occurred during the same period following the Springs Fire (Florsheim et al., 2013). The value measured in Klein Reach (Reach A) is also smaller than volumes measured following other wildfires in the Transverse Ranges; for example after the 1985 Wheeler Fire, post-fire dry ravel contribution before winter flows equaled 0.20 m^3/m. Similarly, a higher value of 0.33 m^3/m was reported following a fire in the Oregon Coast Ranges (Gerber; 2004). The spatial variability in sediment delivery within one basin and among basins in various environments could be related to the proximity, length, and gradient of slopes without soil cover situated directly above the channel; however, further work is warranted to quantitatively address factors that influence dry ravel processes and their effect on landscape change following wildfire.

5.2 Dry-ravel deposit dynamics: changes after initial deposition

Field measurements and TLS scanning provide data quantifying the volume of sediment contributed to a study reach in Big Sycamore Canyon immediately following the Springs wildfire. Moreover, geomorphic changes in these deposits occur after the initial pulse; the results documenting changes in dry ravel deposits highlight processes of erosion and deposition within individual deposits during a storm season with one small runoff-generating storm. Dry-ravel deposits occur in the hillslope-channel margin transition zone influenced by upslope hillslope processes, and by channel fluvial processes. After wildfire burns stabilizing vegetation, hillslopes supply available weathered sediment via dry ravel processes to a zone of hillslope-channel interaction—the area at the base of hillslopes at the margin of seasonally dry channels. Moreover, our results illustrate that sediment in storage on channel-margin dry-ravel deposits formed during or immediately after wildfires exists near the angle of repose—leading to erosion and deposition processes within individual deposits after the initial post-fire pulse. For example, erosion on the upper portion of deposits and deposition on the lower portions occurred in some of the deposits (see example Figure 10, deposit A01).

Total removal of dry-ravel deposits by fluvial processes has been reported in other post-wildfire investigations (Florsheim et al, 1991; Keller et al., 1997) following moderate storm flows that easily mobilize relatively fine-grained sediment contributed by dry-ravel processes in the Chaparral. In ungaged Big Sycamore Creek, the one small runoff-generating storm that occurred on February 28-March 2, 2014 was not of sufficient magnitude or duration to remove all of the material supplied following the Springs wildfire. Instead, our field investigation indicates that

the six individual deposits with the majority or entirety of their sediment removed account for only ~10% of the reduction of the post-wildfire volume measured in 2013 in the Klein (*Reach A*). We surmise that these deposits were eroded by fluvial processes which undercut and then destabilized the material above until the sediment was removed by channel flow. Continuing longer-term measurements will ultimately reveal the time scales and magnitudes of storms needed to transport or "flush" all of the fire-related ravel deposits downstream. Fluvial processes also appear to be responsible for partial removal of sediment in four deposits by undercutting (A8, A12, A14, A23; see example in Figure 8a). We infer that the majority of sediment in these deposits remained in place because of the small magnitude and duration of the flow event and that future larger storm flows may easily remove the remaining material.

Hillslope processes may continue to influence dry ravel deposits by supplying additional sediment. Four deposits (A05, A13, A14, A17) showed deposition in the upslope portion of their profiles suggesting addition of sediment supplied from hillslopes. Hillslopes may also influence dry-ravel deposits by contributing concentrated overland flow during storms. Small rills with lateral levees that formed in deposits following the February 28-March2, 2014 storm suggest that hillslope-flow pathways continued onto fan surfaces before water percolated into the ravel deposits. Rilling processes account for sediment transport downslope on fan surfaces on three deposits (A15, A16, A22; see example in Figure 8b). Although post-wildfire rills are commonly identified on hillslopes in association with hydrophobic soil layers where a waxy substance is formed within soil (Moody et al., 2013) their presence on porous unconsolidated dry ravel deposits formed as a result of post-wildfire hillslope erosion warrants further investigation. For example, it is unknown if dry ravel deposits inherit some cohesion from grains coated with clay from weathering of local shale deposits, or from the waxy material formed during the wildfire that adheres to grains transported downslope.

Finally, erosion of dry ravel deposits by mass wasting occurs when the shear strength (e.g., frictional resistance, factors causing cohesion of grains, or surface tension caused by moisture) of the deposit decreases below the shear stress on aggregates of grains. Shear stress increases with increasing slope, and small mass-wasting features initiated in over-steepened portions of the dry ravel deposits may cause transfer of sediment farther down the profile of the deposit. Sediment stored on the dry ravel deposits exists near the angle of repose, usually between 30-45° for dry unconsolidated gravel-sized sediment, facilitating erosion and deposition processes that occurred within all of the individual deposits. In addition, disturbances such as small animals running across the deposit or other external factors could trigger mass wasting on the surface of the deposit. Deposition of this mobilized sediment then takes place in micro depressions on the surface or at the base of the deposit.

6. Conclusions

In this paper we present results that combine detailed field measurements and Terrestrial LiDAR Scans illustrating a multi-method approach to measure small changes on dry ravel deposits that aid in understanding geomorphic processes that alter the form of these deposits. This study also addresses sediment dynamics within dry ravel deposits aver initial deposition. For example, after initial deposition following wildfire, alteration of dry ravel deposits formed in the zone of hillslope-channel interaction includes both erosion (~26 %) and deposition (~31%) along the surfaces of these deposits over a seven month period between two TLS field campaigns. Erosion processes include fluvial erosion, rilling, and mass wasting along with continued movement of dry ravel sediment on deposits near the angle of repose. Deposition results when there is a continued supply from the hillslope above and when geomorphic processes transfer dry ravel sediment further down the deposit. Interactions among these processes are influenced by short-term climate variation, hillslope runoff, and channel flow characteristics.

Individual dry ravel deposits distributed irregularly at the margins of stream channels are spatially diffuse and are individually small; however, at the landscape scale, dry ravel processes may dominate post-wildfire sediment yields. Therefore, dry ravel dynamics have implications for a range of issues associated with erosion and sedimentation such as flood hazards, water quality, and ecology.

Acknowledgements

Funding for this work was provided by NSF Rapid EAR-1359734. Terrestrial LiDAR Scans were collected by UNAVCO in support of this grant; we greatly appreciate the work conducted by Ken Austin and Keith Williams toward this effort. We thank Jamie King, Suzanne Goode, and Craig Sap (California State Department of Parks and Recreation) and Martha Witter (National Park Service) for their interest, support, and facilitation of our research in Big Sycamore Canyon. We also appreciate interesting discussion of dry ravel processes and support of this work from Ed Keller, UCSB. The paper was improved by comments and suggestions from Bruce Rhoads, UI, and an anonymous reviewer. Field data collection was aided by talented and energetic students

from UCSB: Michael Ackel, Karla Cortes, and Whitney Jones and from CSUCI: Amber Baglietto, Dylan Ellis, and Alex Gaskill.

References

Anderson H., Coleman G., Zinke, P.J., 1959. Summer slides and winter scour: dry-wet erosion in southern California mountains. USDA Forest Service Technical Paper PSW-36, Pacific Southwest Forest and Range Experimental Station, Berkeley, California, USA.

Benda, L., Dunne, T., 1997. Stochastic forcing of sediment supply to channel networks from landsliding and debris flow. *Water Resources Research*, *33*(12):2849-2863.

Chin, A., 1999. The morphologic structure of step-pools in mountain streams. *Geomorphology* 27:191-204.

Chin, A., 2002. The periodic nature of step-pool mountain streams. *American Journal of Science* 302:144-167.

DiBiase, R.A. and Lamb, M.P., 2013. Vegetation and wildfire controls on sediment yield in bedrock landscapes. Geophysical Research Letters 40:1093-1097 doi:10.1002/grl.50277, 2013.

Dibblee, T.W., and Ehrenspeck, H.E., 1990a. Geologic map of the Point Mugu and Triunfo Pass quadrangles, Ventura and Los Angeles Counties, California. Map Scale: 1:24,000. Dibblee Foundation Map DF-29.

Dibblee, T.W., and Ehrenspeck, H.E, 1990b. Geologic map of the Camarillo and Newbury Park quadrangles, Ventura County, California. Map Scale: 1:24,000. Dibblee Foundation Map DF-28.

DeBano, L.F., Rice, R.M., Conrad, C.E., 1979. Soil heating in chaparral fires; effects on soil properties, plant nutrients, erosion and runoff: U.S. Forest Service Research Paper PSW-145, 21p.

Florsheim, J.L., Keller, E.A., Best, D.W., 1991. Fluvial sediment transport in response to moderate storm flows following chaparral wildfire, Ventura County, southern California. *Geological Society of America Bulletin* 103, 504–511.

Florsheim, J.L., Chin, A., O'Hirok, L.S., Keller, E.A., 2013. Effect of chaparral wildfire on dry ravel processes. *Geological Society of America, Abstracts With Programs*. Vol. 45, No. 7.

Gabet, E.J., 2003. Sediment transport by dry ravel. *Journal of Geophysical Research: Solid Earth* 1978–2012:108(B1).

Gabet, E.J., Dunne, T., 2003. A stochastic sediment delivery model for a steep Mediterranean landscape. *Water Resources Research 39*(9).

Gerber, M., 2004. Geomorphic response to wildfire in the Oregon Coast Range [M.S. thesis]: Eugene, University of Oregon, 94 p.

Kean J.W., Staley, D.M., Cannon, S.H., 2011. In situ measurements of post-fire debris flows in southern California: Comparisons of the timing and magnitude of 24 debris-flow events with rainfall and soil moisture conditions. *Journal of Geophysical Research* VOL. 116, F04019, doi:10.1029/2011JF002005, 2011.

Keller, E.A., Valentine, D.W., Gibbs, D.R., 1997. Hydrological response of small watersheds following the southern California Painted Cave fire of June 1990. *Hydrological Processes* 11:401-414.

Krammes, J.S., 1965. Seasonal debris movement from steep mountainside slopes *in* southern California, in proceedings, Federal Inter-Agency Sedimentation Conference, Jackson, Miss.: US Department of Agriculture Miscellaneous Publications, v. 970, p. 85-88.

Lamb, M.P., Scheingross, J.S., Amidon, W.H., Swanson, E., Limaye, A., 2011. A model for fire-induced sediment yield by dry ravel in steep landscapes. *Journal of Geophysical Research: Earth Surface* VOL. 116, F03006, doi:10.1029/2010JF001878, 2011.

Lamb, M.P., Levina, M., DiBiase, R.A., Fuller, B.M., 2013, Slope, roughness and particle-size controls on sediment storage by vegetation in steep bedrock landscapes: Theory, experiments and implications for post-fire sediment yield. *Journal of Geophysical Research: Earth Surface*, doi:10.1002/jgrf.20041.

Lavé, J., Burbank, D., 2004. Denudation processes and rates in the Transverse Ranges, southern California: Erosional response of a transitional landscape to external and anthropogenic forcing. *Journal of Geophysical Research: Earth Surface 2003*–2012:109(F1).

Moody, J.A. Martin, D.A, 2009. Synthesis of sediment yields after wildland fire in different rainfall regimes in the western United States. *International Journal of Wildland Fire* 18:96–115.

Moody, J.A., Shakesby, R.A., Robichaud, P.R., Cannon, S.H., Martin, D.A., 2013. Current research issues related to post-wildfire runoff and erosion processes. *Earth Science Reviews* http://dx.doi.org/10.1016/j.earscirev.2013.03.004.

Moritz, M.A., Moody, T.J., Krawchuck, M.A., Hughes, M., Hall, A., 2010. Spatial variation in extreme winds predicts large wildfire locations in chaparral ecosystems. *Geophysical Research Letters* Vol. 37, L04801, doi:10.1029.2009GL041735, 2010.

Morris S.E., Moses, T.A., 1987. Forest fire and the natural soil erosion regime in the Colorado Front Range. *Association of American Geographers, Annals* 72:245-254.

National Park Service (NPS), 2013. Burned Area Emergency Response Plan (BAER), Springs Fire, May2-May 12, 2013. National Park Service, U.S. Department of the Interior, Pacific West Region. Report prepared by the National Park Service Springs Fire BAER Team, 216 p.

O'Leary, J.F., 1981. Native vegetation of the Santa Monica Mountains, *in* Logan, R. F., ed., Field trip guide, Los Angeles Meeting, 1981: Assoc. Am. Geog., p. 95–98.

Quinn, R.D., and Keeley, S.G., 2006. Introduction of California Chaparral. University of California Press, Berkeley, CA. 322p.

Rice, R.M., 1974. The hydrology of chaparral soils, *in* Proceedings, Symposium on Living with the Chaparral: Riverside, California, Sierra Club, p. 27-34.

Rice, R. M., Sedimentation in the chaparral: How do you handle unusual events?, in Sediment Budgets and Routing in Forested Drainage Basins, edited by F. J. Swanson et al., pp. 39– 49, For. Serv. U.S. Dep. Agric., Washington, D. C., 1982.

Roering, J.J., Gerber, M., 2005. Fire and the evolution of steep, soil-mantled landscapes. *Geology*, *33*(5):349-352.

Scott K.M., Williams, R.P., 1978. Erosion and sediment yields in the Transverse Ranges, southern California: *U.S. Geological Survey Professional Paper* 1030, 37 p.

Shakesby, R.A., Doerr, S.H., 2006. Wildfire as a hydrological and geomorphological agent. *Earth Science Reviews* 74: 269–307.

Williams, K.E., Olsen, M.J., Chin, A., 2012. Accuracy Assessment of Geo-Referencing Methodologies for Terrestrial Lidar Laser Scan Site Surveys. American Society for Photogrammetry & Remote Sensing (ASPRS) Annual Conference, Sacramento, California, March 19-23. 2012, 10p.

Yerkes, R.F., Campbell, R.H., Alvarez, Rachel, and Bovard, Kelly, 2005. Preliminary geologic map of the Los Angeles 30' X 60' quadrangle, southern California. Map Scale: 1:100,000. U.S. Geological Survey, Open-File Report OF-2005-1019.

Yerkes, R. F., and Campbell, R. H., 1980, Geological map of east-central Santa Monica Mountains, Los Angeles County, California: U.S. Geol. Survey Misc. Invest. Series, Map I-1146, Map Scale 1:24,000.

Westerling, A.L., Hidalgo, H.G., Cayan, D.R., Swetnam, T.W., 2006. Warming and earlier spring increase western U.S. forest wildfire activity. *Science* 313, 940 (2006) DOI: 10.1126/science.1128834.

Figures

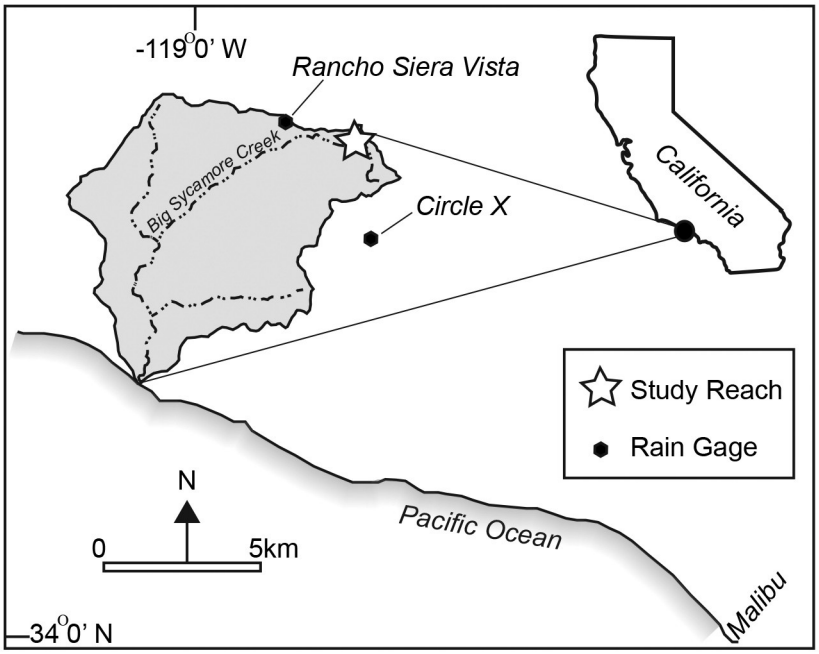

Figure 1. Map showing location of study reach in Big Sycamore Canyon and nearby rain gages.

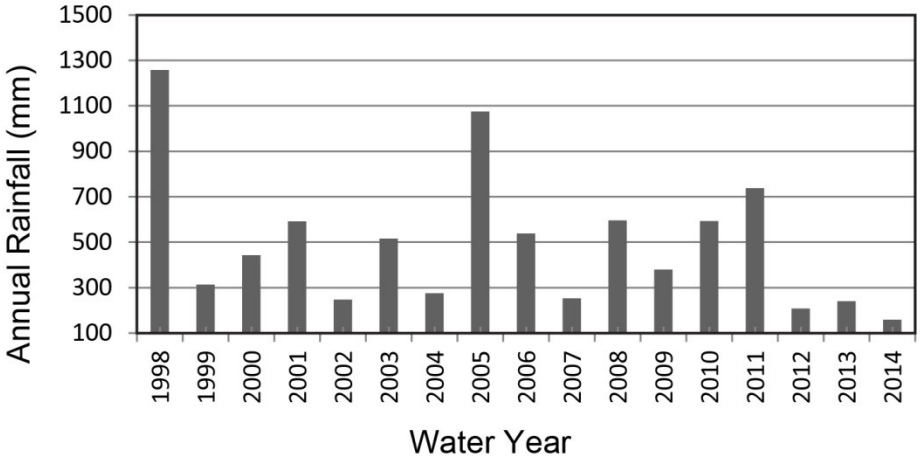

Figure 2. Annual rainfall for nearby Circle X precipitation station illustrating three-year drought conditions. Gage is located over in Malibu Creek watershed, immediately east of Big Sycamore Canyon. Data source: Ventura County Watershed Protection District (2014a).

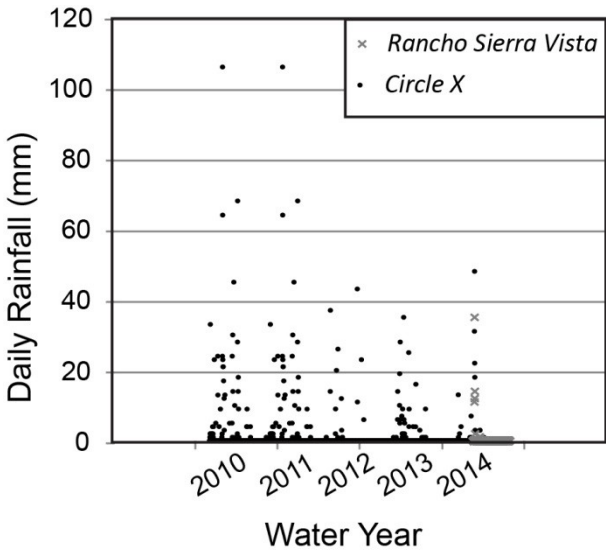

Figure 3. Daily rainfall during water year 2010-2014 for nearby Circle X rain gage. Also shown are data available from the Sierra Vista rain gage (data available since February 2014; Ventura County Watershed Protection District, 2014a and 2014b).

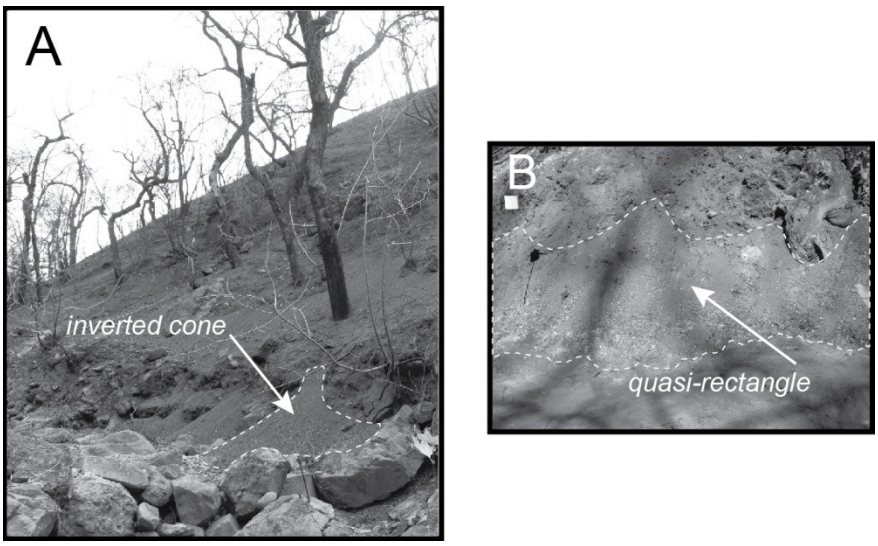

Figure 4. Photos: examples of dry ravel deposit morphology. 4a. Inverted cone-shaped deposit. 4b. Irregular, quasi-rectangular-shaped deposit.

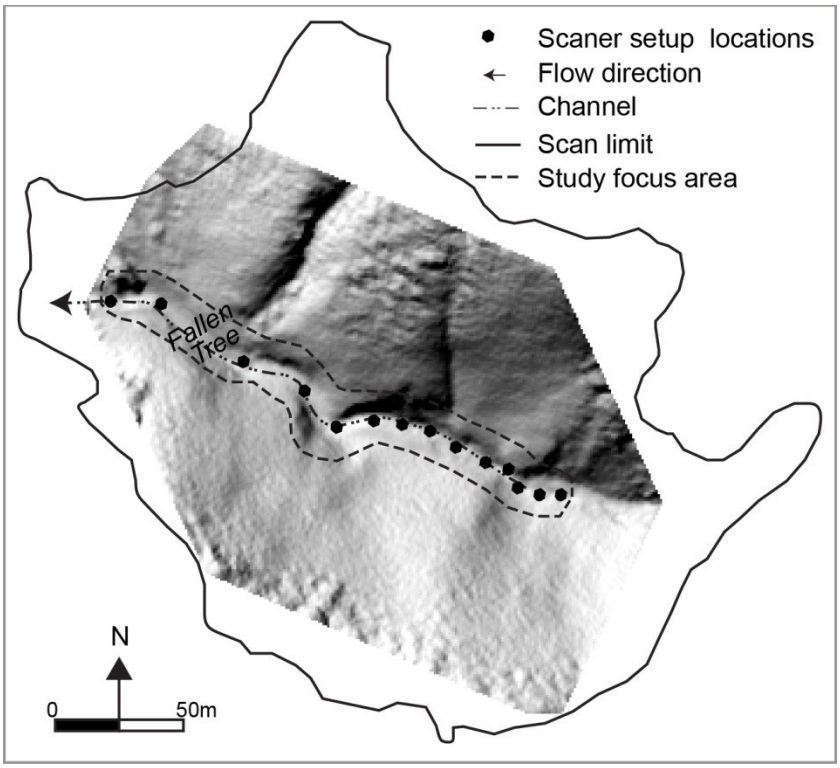

Figure 5. Base map showing Terrestrial LiDAR scanner set up locations along Klein Reach (*Reach A*). The hillshade background on the basemap was generated in ArcGIS using coarse topographic filtering (approximately 1 point per 5 meters).

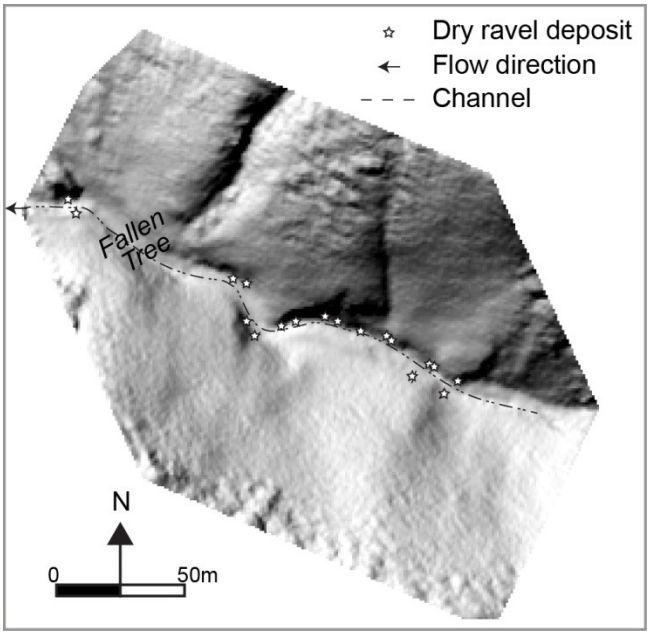

Figure 6. Spatial distribution of dry ravel deposits in Klein Reach (Reach A)

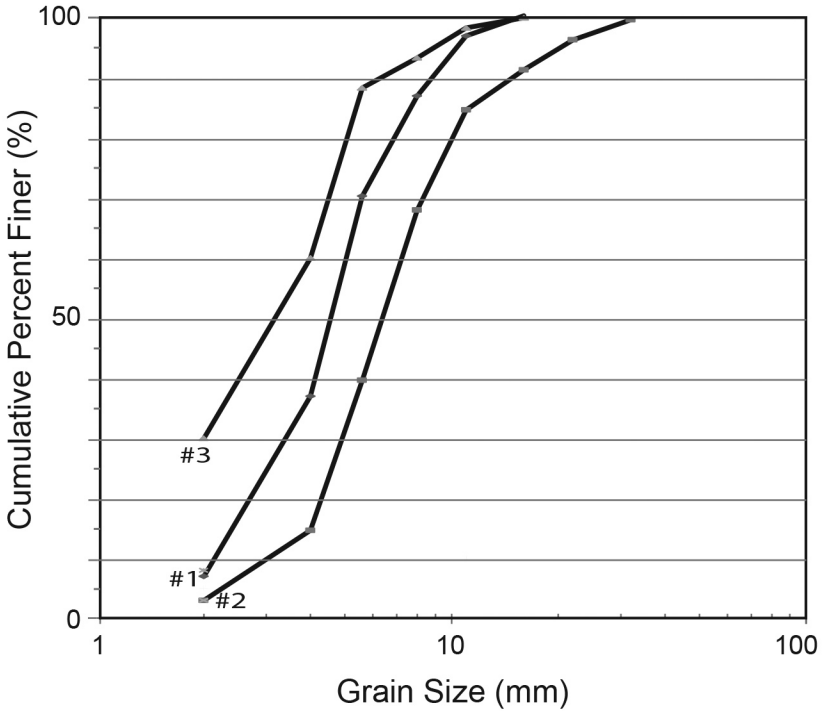

Figure 7. Grain size distributions of sediment contributed by dry ravel in Klein Reach (Reach A).

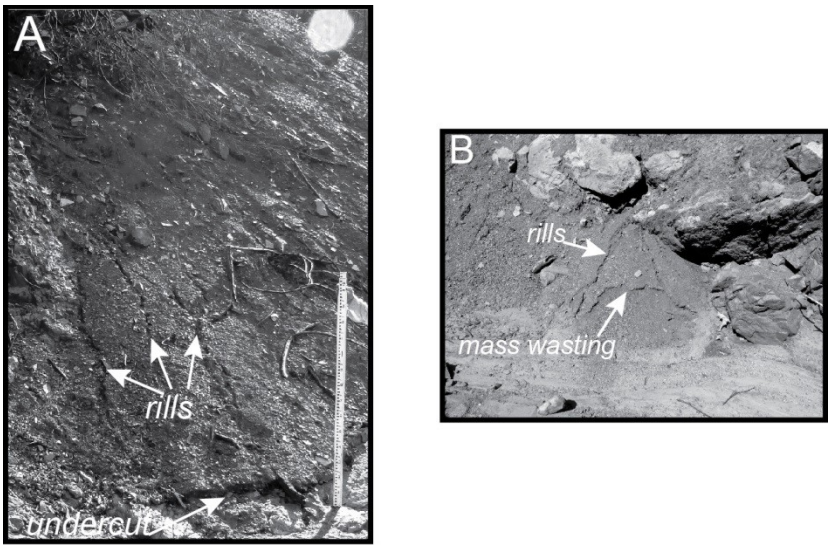

Figure 8. Photos: processes that contributed to the reduction of sediment stored in dry ravel. 8a. Undercutting at the base of a deposit by fluvial erosion and small rills formed in the surface of the deposit. 8b. Rill and small mass wasting failure in the surface of the deposit.

a)

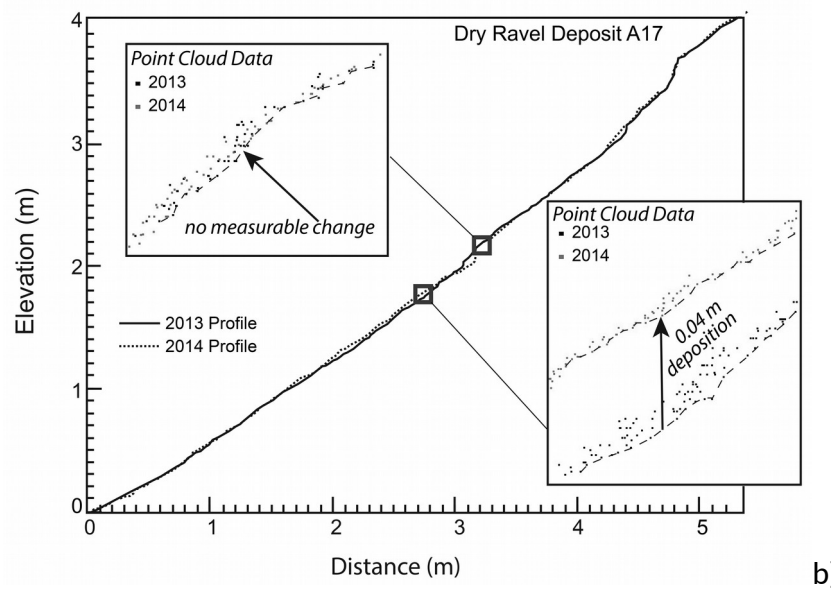

b)

Figure 9. 9a. Photograph showing dry ravel deposit and location of profile analyzed (17A). 9b. Corresponding profile constructed using TLS point cloud data to quantify changes in erosion and/or deposition of sediment along a dry ravel deposit profile scanned in 2013 and 2014. Inset boxes display examples of highly magnified point cloud data analyzed to generate profiles showing no measurable change (upper box) or deposition (lower box) between the 2013 and 2014 TLS field campaigns (profiles were drawn though the lowest points in the point cloud along the profile).

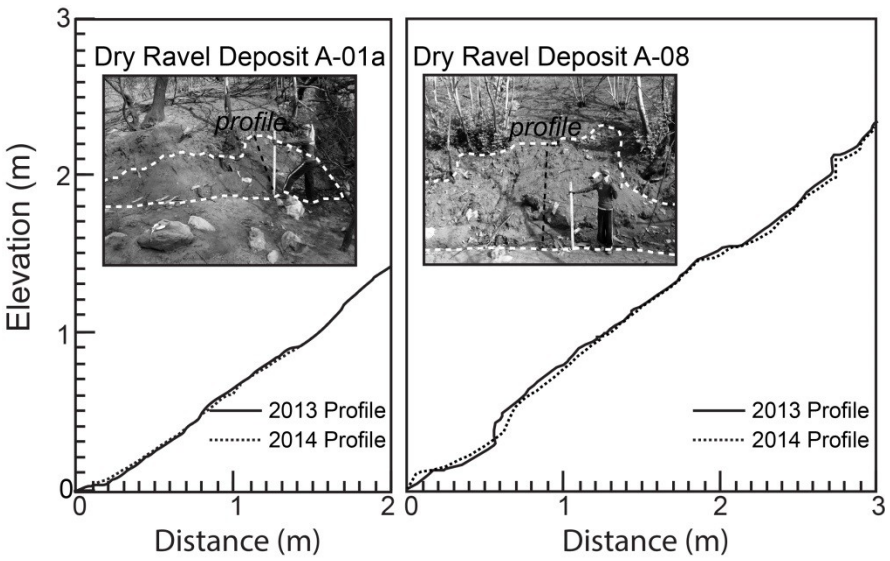

Figure 10. Examples showing 2013 and 2014 profiles for dry ravel deposits A01 and A08. Photographs showing deposits were taken in March 2014 after the storm. Profile locations indicated by dashed black line; boundary of deposits indicated by dashed white line.